Domains in Cationic Lipid plus Polyelectrolyte Bilayer Membranes: Detection and Characterization via ^{2}H Nuclear Magnetic Resonance[†]

Peter Mitrakos and Peter M. Macdonald*

Department of Chemistry and Erindale College, University of Toronto, 3359 Mississauga Road North, Mississauga, Ontario, Canada L5L 1A2

Received June 3, 1997; Revised Manuscript Received August 11, 1997[⊗]

ABSTRACT: ^{2}H nuclear magnetic resonance (NMR) spectroscopy of choline-deuterolabeled 1-palmitoyl-2-oleoyl-*sn*-glycero-3-phosphocholine (POPC-α-d_2 and POPC-β-d_2) has been used to detect and quantify domain formation induced in cationic lipid-containing bilayers upon the addition of anionic polyelectrolytes. Three different polyelectrolytes, poly(sodium 4-styrenesulfonate) or PSSS, poly(sodium acrylate) or PACA, and poly(sodium glutamate) or PGLU, were added to POPC lipid bilayers containing 1,2-dioleoyl-3-(dimethylamino)propane (DODAP) as the cationic amphiphile. All three polyelectrolytes produced two-component ^{2}H NMR spectra, consistent with two populations of POPC, one polyelectrolyte-bound and another polyelectrolyte-free. The relative intensities of the two spectral components provided the relative amounts of the two POPC populations. The ^{2}H NMR quadrupolar splitting from either spectral component provided the DODAP content of the particular POPC population. The two POPC populations differed in that the polyelectrolyte-bound population contained a stoichiometric polyelectrolyte anion:DODAP cation ratio leading to enrichment with respect to DODAP, while the polyelectrolyte-free population was depleted of DODAP. Estimates of the size of a polyelectrolyte-defined domain revealed a constant number of bound DODAP but a flexible number of bound POPC, which increased in proportion to the global POPC content. The most compact domains were formed by the most hydrophobic polyelectrolyte, PSSS, while the most expansive domains were formed by the most hydrophilic polyelectrolyte, PGLU.

Domains in biological membranes have become the focus of considerable interest [for recent reviews see Thompson et *al.* (1992), Vaz (1992), Glaser (1992), Tocanne (1992), Edidin (1992), Wolf (1992), and Jesaitis (1992)]. An in-plane domain consists of a region of distinct composition, having significant dimension and duration. The two foremost and immediate challenges in the study of in-plane domains are to understand their physical origin and to assess their functional significance. Membrane macrodomains, on the order of 1 μm in size, are associated with protein−protein interactions, such as those between the cytoskeletal protein spectrin and red blood cell membrane proteins (Bennet, 1985). Lipid−protein interactions, such as the electrostatic attraction between cytochrome *c* and anionic phospholipids [e.g., de Kruijff and Cullis (1980)], yield microdomains capable of aggregating into macrodomains (Haverstick & Glaser, 1989). Microdomains, on the nanometer scale, are associated as well with lipid−lipid interactions, such as occur in cases of nonideal mixing of different lipid species [e.g., Mabrey and Sturtevant (1976)]. In only a few instances is it possible to state with confidence the functional significance of particular domain structures. Likewise, there is a paucity of molecular-level detail regarding domain formation, distribution, and dissolution.

Part of the difficulty is that each method for observing in-plane membrane domains has unique advantages and disadvantages, so that "the domain is in the eye of the beholder". For instance, the remarkable images of macroscopic domains obtained via fluorescence digital imaging microscopy [e.g. Luan *et al.* (1995)] allow one to assess domain size and shape but not the details of domain composition. Fluorescence recovery after photobleaching (FRAP) permits one to extract domain shape information from the observed percolation threshold, provided the phase diagram for the system of interest is already available (Jovin & Vaz, 1989). Diffraction (Blasie *et al.*, 1985) and calorimetric (McElhaney, 1982) methods provide global assessments of domain structure from which phase diagrams may be constructed but provide little molecular-level insight, although they have the virtue of using intrinsic probes, thereby avoiding any question of probe-induced perturbations. Spectroscopic techniques, such as fluorescence spectroscopy (Davenport *et al.*, 1989) or electron spin resonance (ESR) of appropriately labeled probe molecules [e.g., Zachowski and Devaux (1983)] have provided an abundance of molecular-level information regarding domain composition and properties. NMR spectroscopy, on the other hand, has added little to the study of in-plane domains, at least in comparison to its decisive contributions to the understanding of other fundamentals of membrane molecular structure and dynamics. Phosphorus (^{31}P) NMR, for example, is used to examine the macroscopic architecture of the membrane lipids, i.e., bilayer versus hexagonal H_{II} versus isotropic or cubic arrangements (Seelig, 1978; Cullis & de Kruijff, 1979), but it is difficult to specify the origin of the signal when two or more phospholipids are present simultaneously. Deuterium (^{2}H) NMR, while having an enormous impact on the understanding of many aspects of membrane biophysical chemistry (Seelig, 1977; Seelig & Seelig, 1980; Davis, 1983),

[†] This work was supported by a National Science and Engineering Research Council (NSERC) of Canada Operating Grant (P.M.M.).

* Author to whom correspondence should be addressed: Tel 905-828-3805; Fax 905-828-5425; E-mail: pmacdona@credit.erin.utoronto.ca.

[⊗] Abstract published in *Advance ACS Abstracts,* October 1, 1997.

S0006-2960(97)01324-X CCC: $14.00

generally fails to resolve in-plane domains observed with other spectroscopic techniques. In all likelihood this is due to differences in the characteristic time scales of the different spectroscopic methods versus the lifetimes of the domains (Bloom & Thewalt, 1995).

Recently, we reported the first use of ^{2}H NMR to detect in-plane bilayer membrane domains formed in model charged lipid bilayers exposed to oppositely charged polyelectrolytes (Mitrakos & Macdonald, 1996; Crowell & Macdonald, 1997). The ability to resolve such domains relies on the sensitivity of the ^{2}H NMR spectrum of choline-deuterolabeled phosphatidylcholine to lipid bilayer surface electrostatic charge (Seelig *et al.*, 1987) and the differences in surface charge between different domains of different composition. The initial lipid bilayer surface charge can originate with cationic lipids, such as those employed in gene transfection techniques (Felgner & Rhodes, 1991), or anionic lipids, such as naturally occurring phosphatidylglycerol. An anionic polyelectrolyte, like DNA (Mitrakos & Macdonald, 1996), produces effects similar to a synthetic cationic polyelectrolyte, like poly(vinylbenzyltrimethylammonium chloride) (PVTA) (Crowell & Macdonald, 1997), demonstrating the predominantly electrostatic origin of the domain formation in such cases. In both situations, we observe polyelectrolyte-containing domains enriched with oppositely charged lipids in coexistence with polyelectrolyte-free domains depleted of oppositely charged lipids. Analysis of the ^{2}H NMR spectra permits a facile assessment of the degree of domain formation, the domain composition, the molecular dynamics within domains, and a lower limit on the domain size.

The value of such studies of model, synthetic membrane systems resides in the capacity to manipulate at will the physicochemical variables of relevance and to observe their impact on the resulting domains. In this report we describe ^{2}H NMR studies comparing the ability of three synthetic anionic polyelectrolytes to produce domains in lipid bilayers consisting of mixtures of the cationic lipid 1,2-dioleoyl-3-(dimethylamino)propane (DODAP) with the zwitterionic lipid 1-palmitoyl-2-oleoyl-*sn*-glycero-3-phosphocholine (POPC), specifically deuterolabeled in its choline head group. The three polyelectrolytes, poly(sodium 4-styrenesulfonate) or PSSS, poly(sodium acrylate) or PACA, and poly(sodium glutamate) or PGLU, differ primarily with respect to the hydrophobicity of their polymer backbones, ranging from very hydrophobic (PSSS) to exceedingly hydrophilic (PGLU). This permits an evaluation of the relative contribution of electrostatic and hydrophobic considerations to sequestration of cationic lipids into polyelectrolyte-containing domains. We demonstrate that all three species are able to induce in-plane domain formation but that the detailed composition and size of the domains so produced depends on the hydrophilic/lipophilic balance of the polyelectrolyte.

MATERIALS AND METHODS

Materials. 1-Palmitoyl-2-oleoyl phosphatidic acid (POPA) and nondeuterated POPC were purchased from Avanti Polar Lipids (Alabaster, AL). Poly(L-glutamic acid) sodium salt (PGLU, MW 80 000, degree of polymerization $N = 550$) and oleoyl chloride were obtained from Sigma (St. Louis, MO). Poly(acrylic acid), sodium salt (PACA, MW 30 000, $N = 320$), poly(sodium 4-styrenesulfonate) (PSSS, MW 70 000, $N = 340$), sodium tetraphenylboron (TPB), 2,3,4-triisopropylbenzenesulfonyl chloride (TPS), 3-(dimethylamino)-1,2-propanediol, and deuterium-depleted water were purchased from Aldrich (Milwaukee, WI).

Synthesis of Choline-Deuterated Phosphatidylcholine. 1-Palmitoyl-2-oleoyl-*sn*-glycero-3-phosphocholine (POPC) was selectively deuterated at either the α or β positions of the choline head group using a strategy based on a combination of the methods of Harbison and Griffin (1984) and Aloy and Rabout (1913). In short, POPC-α-d_2 and POPC-β-d_2 were synthesized by coupling the tetraphenylboron salts of the corresponding choline head groups to POPA, using TPS as the condensing agent (Aneja *et al.*, 1970). The deuterated phosphatidylcholines were then purified by elution through an Amberlite mixed-bed ion exchanger (BDH, Toronto, ON), followed by acetone precipation. The purity of the lipids was determined by thin-layer chromatography (TLC) and by ^{1}H and ^{2}H NMR.

Synthesis of DODAP. 1,2-Dioleoyl-3-(dimethylamino)-propane (DODAP) was synthesized and purified as described by Leventis and Silvius (1990). Briefly, 3-(dimethylamino)-1,2-propanediol was coupled with oleoyl chloride to produce DODAP. The product was then purified by dissolving it in 99:1 (v/v) hexane/acetic acid, applying this mixture to a silicic acid column, and eluting successively with 20% diethyl ether in hexane, 100% chloroform, and finally, 10% methanol in chloroform. DODAP eluted as its acetic acid salt with the 10% methanol fraction. DODAP was then converted to its hydrochloride salt by addition of an equimolar amount of HCl to a methanolic solution of DODAP. Methanol was then removed under a stream of argon gas and the product was further dried under vacuum overnight. The purity of the lipid was confirmed by TLC and ^{1}H NMR. TLC yielded a single spot with $R_f = 0.70$ when chromatographed in chloroform:methanol (90/10 v/v). Proton NMR results have been reported elsewhere (Mitrakos & Macdonald, 1996).

Synthesis of Amino-Deuterated DOTAP. 1,2-Dioleoyl-3-(trimethylamino)propane deuterated in one of its aminomethyls (DOTAP-γ-d_3) was synthesized from DODAP using methyl-d_3 iodide (Aldrich, Milwaukee, WI) essentially as described by Macdonald *et al.* (1991) for related species. The amino-deuterated DOTAP was purified and characterized as described for DODAP.

Preparation of Multilamellar Vesicles (MLVs). Lipid mixtures of the desired composition were prepared by combining the appropriate volumes of chloroform stock solutions of either POPC-α-d_2 or POPC-β-d_2 with that of DODAP. Typically, the lipid mixtures consisted of 10 mg of the desired deuterated POPC along with varying amounts of DODAP, in order to achieve the prescribed lipid molar ratio. The solvent was removed under a stream of argon and the mixture was dried overnight under vacuum. The dried lipids were then rehydrated in 160 mL of deuterium-depleted water. The hydration process consisted of gentle warming and vortexing, followed by five cycles of freeze−thaw to ensure lipid mixing.

Preparation of MLVs Containing Polyelectrolytes. The dried lipid mixtures were prepared as described above but were hydrated using deuterium-depleted water containing the desired amount of either PSSS, PACA, or PGLU. Sufficient deuterium-depleted water was added to bring the final volume to 160 mL. The solution was then gently warmed and vortexed and subjected to five freeze−thaw cycles to ensure homogeneous mixing.

NMR Measurements. ^{2}H NMR spectra were recorded on a Chemagnetics CMX300 NMR spectrometer operating at 45.98 MHz, using a Chemagnetics wide-line deuterium probe. The quadrupolar echo sequence (Davis *et al.*, 1976) was employed using quadrature detection with complete phase cycling of the pulse pairs, a 90° pulse length of 1.9 ms, an interpulse delay of 30 μs, a recycle delay of 100 ms, a spectral width of 100 kHz, and a 2K data size.

^{31}P NMR spectra were recorded on the same spectrometer operating at 121.25 MHz, using a Chemagnetics double-resonance magic-angle spinning (MAS) probe but without sample spinning. The Hahn echo sequence with complete phase cycling of the pulses and proton decoupling during acquisition was employed as described by Rance and Byrd (1983). The 90° pulse length was 6.5 μs, the echo spacing was 40 μs, the recycle delay was 2 s, the spectral width was 100 kHz, and the data size was 2K. All ^{2}H and ^{31}P NMR spectra were recorded at room temperature.

Pake Pattern Spectral Line-Shape Simulations. ^{2}H NMR Pake pattern line shapes were simulated using a computer program, written in our laboratory, based on the tiling method introduced by Alderman *et al.* (1986). The simulation variables include the quadrupolar splitting, $\Delta\nu$, the line width parameter, T_2, and the intensity of a given Pake pattern. The program does not include provisions for T_2 asymmetry effects. This can sometimes lead to less-than-perfect simulations, particularly evident in the spectral shoulders.

Difference Assay of Polyelectrolyte-Membrane Binding. Dried lipid samples were prepared as described above, except that nondeuterated POPC was employed, and the desired amount of either PSSS, PACA, or PGLU was added from an aqueous stock solution. The final volume of the mixture was brought to 300 μL and the samples were then hydrated and equilibrated as above. The mixtures were then centrifuged at 13 000 rpm for 30 min to pellet the lipid bilayers. The supernatant was decanted and any unpelleted lipid was eliminated with using a Centricon-30 microconcentrator (Amicon, Oakville, ON). The supernatant was diluted until its UV absorbance, measured with a Hewlett-Packard 8452A diode array spectrophotometer, fell into the concentration regime where Beer's Law is obeyed for the particular polyelectrolyte, and the polyelectrolyte concentration was calculated from a standard curve.

RESULTS AND DISCUSSION

General Properties of Cationic Lipid Bilayers Exposed to Anionic Polyelectrolytes. The structures of DODAP, a cationic amphiphile, and POPC, a zwitterionic amphiphile, are illustrated in Figure 1, along with the nomenclature of the relevant deuterium labeling positions. Aqueous mixtures of DODAP plus POPC spontaneously assemble into lipid bilayers, as opposed to some other architecture such as an hexagonal H_{II} or isotropic or cubic arrangement, at all proportions of the two examined here. The ^{31}P NMR spectrum on the top left in Figure 3 demonstrates this point for the case of a 20/80 (mol/mol) DODAP + POPC mixture, in that its line shape is diagnostic of lipids in a bilayer arrangement (Seelig, 1978; Cullis & de Kruijff, 1979). (Throughout this paper all proportions of lipid mixtures will be presented as molar ratios.)

The structures of the repeating unit of the three anionic polyelectrolytes examined in this study are also shown in Figure 1. Of the three, PGLU is clearly the most hydrophilic, since its polymeric backbone consists of a peptide chain. In

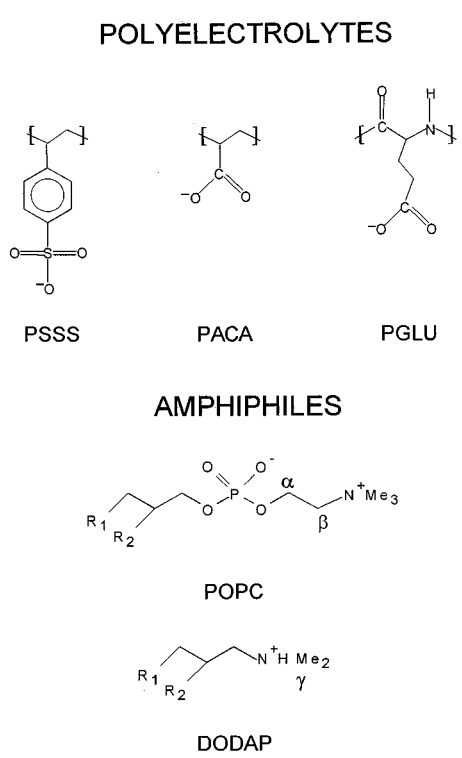

FIGURE 1: Chemical structure of the three anionic polyelectrolytes (PSSS, PACA, and PGLU), the zwitterionic amphiphile (POPC), and the cationic amphiphile (DODAP) employed here. The Greek letters α, β, and γ designate the various deuteron-labeling positions in POPC and DODAP. The nominal degree of polymerization (N) is 340 for PSSS, 320 for PACA, and 550 for PGLU.

comparison, the ethylenic backbone of PACA or PSSS is relatively hydrophobic. When the aromatic ring of PSSS is considered, it is evident that one may arrange these three polyelectrolytes in order of increasing hydrophobicity as follows: PGLU < PACA < PSSS.

When any of these anionic polyelectrolytes are added to the aqueous medium with which the DODAP + POPC mixtures are hydrated, the dispersions so produced exhibit colloidal properties markedly different from those observed in the absence of polyelectrolytes. Specifically, the multilamellar vesicles (MLVs) formed with DODAP + POPC mixtures in the absence of polyelectrolyte are finely dispersed and difficult to centrifuge, due to the intervesicular repulsion arising from the cationic surface electrostatic charge, in accordance with classical DLVO (Derjaguin, Landau, Verwey, and Overbeek) theory of colloidal stability (Derjaguin & Landau, 1941; Verwey & Overbeek, 1948). In the presence of anionic polyelectrolytes, the MLVs clump together and are readily centrifuged, behavior indicative of particle flocculation due to surface charge neutralization and/or bridging between vesicles by the polyelectrolytes (Pefferkorn, 1995). These are macroscopic manifestations of the electrostatic interactions between the anionic polyelectrolytes and the cationic lipid bilayers.

Still on the macroscopic level, the binding of the various anionic polyelectrolytes to cationic lipid bilayers may be quantified using a depletion assay, as described under Materials and Methods. The results, shown in Figure 2, indicate that polyelectrolyte binding is virtually quantitative up to the anion/cation equivalence point. Adding further polyelectrolyte produces further binding to the lipid bilayers, but at a much reduced level relative to the amount added. All three polyelectrolytes behave identically in this respect, within the limits of the precision of the depletion assay.

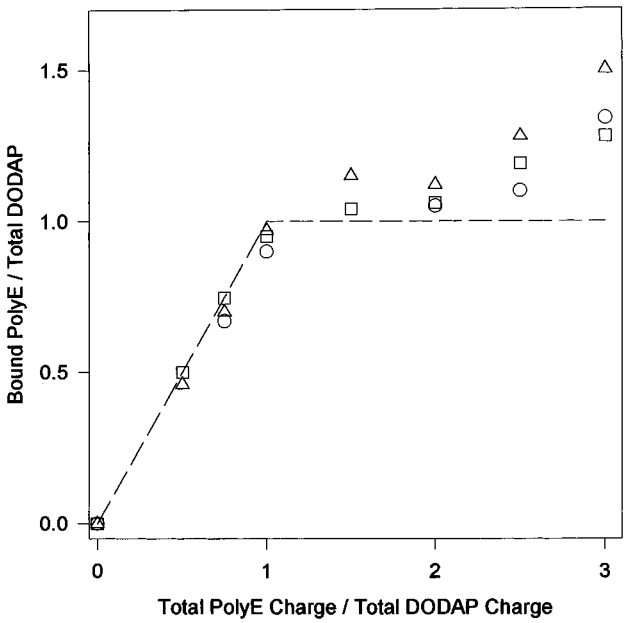

FIGURE 2: Ultraviolet (UV) depletion assay of the extent of polyelectrolyte binding to lipid bilayers composed of DODAP + POPC (10/90 mol/mol) as a function of added PSSS (squares), PACA (circles) or PGLU (triangles). The dashed line indicates the results expected for 100% binding up to the equivalence point, followed by no further binding.

At the equivalence point, where sufficient polyelectrolyte has been added to neutralize the cationic lipid, the lipids retain their overall bilayer arrangement, as demonstrated by the ^{31}P NMR spectrum on the bottom left in Figure 3, which is again diagnostic of phospholipids in a fluid lipid bilayer. Further to this point, when deuteron labels are placed on the polar head group of either the cationic lipid DOTAP or the zwitterionic lipid POPC, the resulting ^{2}H NMR spectra are characteristic of fluid lipids in a bilayer arrangement, both in the absence and in the presence of polyelectrolyte, as shown by the top and bottom row of spectra, respectively, in Figure 3. Thus, despite the binding of polyelectrolyte to the lipid vesicles and the resultant neutralization of surface charge and vesicle flocculation, the assembled lipid molecules maintain a fluid bilayer macroscopic organization.

^{2}H NMR Evidence for Domain Formation by Polyelectrolytes. It is well-known that ^{2}H NMR of choline-deuterolabeled phosphatidylcholine provides a sensitive means of monitoring electrostatic charge at the surface of lipid bilayer membranes (Seelig *et al.*, 1987). The critical features are illustrated in the ^{2}H NMR spectra of POPC-α-d_2 and POPC-β-d_2, shown second from right and rightmost, respectively, in the top row in Figure 3. These spectra were obtained for POPC mixed with 10% or 20% DODAP, for POPC-α-d_2 and POPC-β-d_2 respectively, but in the absence of polyelectrolyte. The quantity measured from such a spectrum is the quadrupolar splitting, $\Delta\nu$, corresponding to the separation, in hertz, between the two maxima or "horns" in the so-called Pake doublet spectral line shape. (The small narrow resonance at 0 Hz in these spectra arises from the residual deuterium present even in deuterium-depleted water.) The values of $\Delta\nu$ measured from these spectra (3000 and 8200 Hz for POPC-α-d_2 and POPC-β-d_2, respectively) differ markedly from the values measured for 100% POPC membranes (6400 and 5800 Hz for POPC-α-d_2 and POPC-β-d_2, respectively). We have demonstrated previously that such changes in $\Delta\nu$ relative to the controls continue in a progressive, linear fashion with increasing mole fraction of added DODAP (Mitrakos & Macdonald, 1996).

This inverse effect of surface charge on the quadrupoplar splitting from the two choline-deuterolabeling positions is characteristic of the so-called "molecular voltmeter" response of phosphatidylcholine (Seelig *et al.*, 1987). The direction of the change in quadrupolar splitting, in this instance, is diagnostic of the presence of cationic surface charges. From the fact that a single quadrupolar splitting is observed for both POPC-α-d_2 and POPC-β-d_2 in the absence of polyelectrolyte, one may deduce that all POPC molecules in the bilayer membranes experience a common surface charge. It follows, therefore, that lipid lateral diffusion within the plane of the two-dimensional bilayer is sufficiently rapid on the ^{2}H NMR time scale (10^{-5}−10^{-6} s) that local deviations from the global mean surface charge are averaged out.

The addition of anionic polyelectrolyte to the cationic lipid bilayers produces two distinct POPC populations observable in the ^{2}H NMR spectrum of choline-deuterated POPC. For instance, as shown on the bottom right in Figure 3, when PSSS is added to mixed DODAP + POPC bilayers in an amount such that there is a global 1:1 PSSS anion:DODAP cation charge ratio, the ^{2}H NMR spectrum consists of a pair of overlapping Pake doublets, for both POPC-α-d_2 and POPC-β-d_2. Similar two-component ^{2}H NMR spectra are produced upon adding any of the three polyelectrolytes PSSS, PACA, or PGLU. The fact that two components are observed in the ^{2}H NMR spectrum indicates that two POPC populations coexist and that any exchange between the two is slow on the time scale defined by the difference in their quadrupolar splittings. Regardless of the deuterolabeling position, one of the component Pake doublets exhibits a quadrupolar splitting greater than the control value, while the second component Pake doublet exhibits a quadrupolar splitting less than the control. This suggests that the two POPC populations produced by adding polyelectrolyte differ with respect to their surface charge, rather than simply, or solely, their respective molecular mobilities. Indeed, it appears from the ^{2}H NMR spectra that both POPC populations retain a high degree of mobility, regardless of any other differences in their local environment.

The ^{2}H NMR spectrum of aminomethyl-deuterated DOTAP consists of a single Pake doublet in the presence of PSSS (second spectrum from left in Figure 3, bottom row). This is not unexpected for two reasons. First, most if not all DOTAP will be associated with polyelectrolyte under these conditions, so that one DOTAP population should predominate. Second, since DOTAP lacks the large dipole moment associated with the zwitterionic phosphocholine head group of POPC, one does not expect a particularly sensitive response to surface charge effects. Rather, one anticipates that the ^{2}H NMR spectrum of DOTAP-γ-d_3 will reflect predominantly local ordering effects. Indeed, it appears that adding PSSS enhances local ordering for the DOTAP head group, a not unreasonable conclusion. DOTAP and DODAP are expected to behave in a rather similar fashion in these circumstances. Detailed studies of the effects of anionic polyelectrolytes on cationic amphiphiles, such as DODAP and DOTAP, will be reported elsewhere.

Further particulars regarding the amount and composition of the polyelectrolyte-induced domains in these mixed DODAP + POPC bilayers are obtainable from a detailed examination of the two ^{2}H NMR quadrupolar splittings and the relative intensities of the two Pake doublets as a function

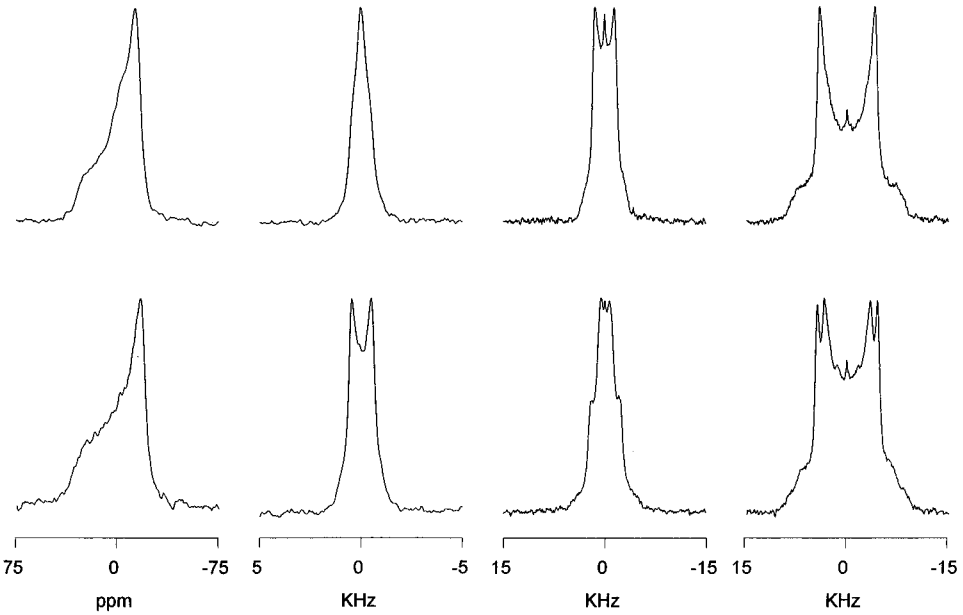

FIGURE 3: NMR spectra of mixed DODAP + POPC cationic lipid bilayers in the absence (top row) and presence (bottom row) of PSSS (1:1 anionic:cationic charge ratio). From left to right, spectra correspond to ^{31}P NMR spectra of DODAP + POPC (20/80), ^{2}H NMR spectra of DOTAP-γ-d_3 + POPC (20/80), ^{2}H NMR spectra of DODAP + POPC-α-d_2 (10/90), and ^{2}H NMR spectra of DODAP + POPC-β-d_2 (20/80).

of added polyelectrolyte. Figure 4 consists of a series of ^{2}H NMR spectra from lipid bilayers composed of mixed DODAP + POPC-α-d_2 (10/90). The four experimental spectra in the top row were obtained upon adding PSSS in the following amounts (from left to right): 0, 0.75, 1.00, and 2.00 equiv of PSSS anions to DODAP cations. Corresponding computer-simulated spectra are arrayed in the bottom row.

From Figure 4 it is evident that, for the case of POPC-α-d_2 mixed with DODAP, adding PSSS produces a two-component ^{2}H NMR spectrum, except at the highest level of PSSS. One Pake doublet displays a quadrupolar splitting smaller than that of the control and grows in intensity with added PSSS. Note that for the case of 0.75 equiv of added PSSS the smaller quadrupolar splitting actually approaches 0 due to the local DODAP concentration. Simultaneously, one observes a second Pake doublet with a quadrupolar splitting greater than that of the control, the intensity of which decreases with added PSSS. This unequivocally identifies the narrower Pake doublet as arising from POPC-α-d_2 associated with added polyelectrolyte. At excess PSSS only a single quadrupolar splitting can be discerned in the spectrum and its value corresponds closely to that of the control measured in the absence of PSSS.

It can be difficult sometimes to judge which of two spectral components is increasing, and which is decreasing, across a series such as shown in Figure 4. Moreover, when two or more Pake doublets overlap in a spectrum, the measured quadrupolar splittings can become distorted from their true values. The computer-simulated spectra shown in the bottom row permit one to extract both the relevant quadrupolar splittings and the relative intensities contributed by the two Pake doublets. The simulations confirm that, in the case of 0.75 PSSS/DODAP charge ratio, the narrower Pake doublet contributes 31% of the POPC-α-d_2 spectral intensity, increasing to 42% at a PSSS/DODAP charge ratio of 1.00.

Figure 5 illustrates the changes observed in the ^{2}H NMR spectrum for the case of lipid bilayers composed of mixed DODAP + POPC-β-d_2 (20/80). As previously, the four spectra, from left to right, were obtained upon addition of PSSS in the following amounts: 0, 0.75, 1.00, and 2.00 equiv of PSSS anions to DODAP cations. Experimentally obtained spectra are arrayed in the top row, while the corresponding computer-simulated spectra are arrayed in the bottom row. Fundamentally the same result is obtained upon addition of PSSS as observed with POPC-α-d_2 in that the spectra consist of a superposition of two main Pake doublet components, one having a larger splitting and the other a smaller splitting than the control. However, for the case of POPC-β-d_2 it is the Pake doublet with the larger quadrupolar splitting that increases in intensity with added PSSS, while that with the smaller splitting decreases in intensity. There is a third, minor component having a narrow quadrupolar splitting and contributing about 5% of the total spectral intensity, which is observed only for the case of PSSS added to bilayers containing POPC-β-d_2. Since no such component was observed in the presence of PACA or PGLU, we have no explanation for its origin. The main points remain that adding PSSS to these cationic bilayers produces a population of POPC-β-d_2 exhibiting a quadrupolar splitting larger than that of the control and that it is this population which increases in intensity upon further additions of PSSS. At excess PSSS levels, the two quadrupolar splittings converge to a single value close to that of the control, as was observed for the case of DODAP + POPC-α-d_2. The corresponding spectral simulations shown in the bottom row confirm these observations and permit a definitive evaluation of both the quadrupolar splittings and the relative intensities of the two main spectral components.

The detailed dependence of the quadrupolar splittings of the two spectral components, polyelectrolyte-bound and polyelectrolyte-free, are shown in Figure 6 for all three polyelectrolytes investigated (PSSS, PACA, and PGLU), and for the two different mixed lipid bilayers, DODAP + POPC-α-d_2 (10/90) (Figure 6A) and DODAP + POPC-β-d_2 (20/80) (Figure 6B). First, it is not possible to resolve two Pake doublets for polyelectrolyte:DODAP ratios less than 0.5 because too little POPC is contained within any domains

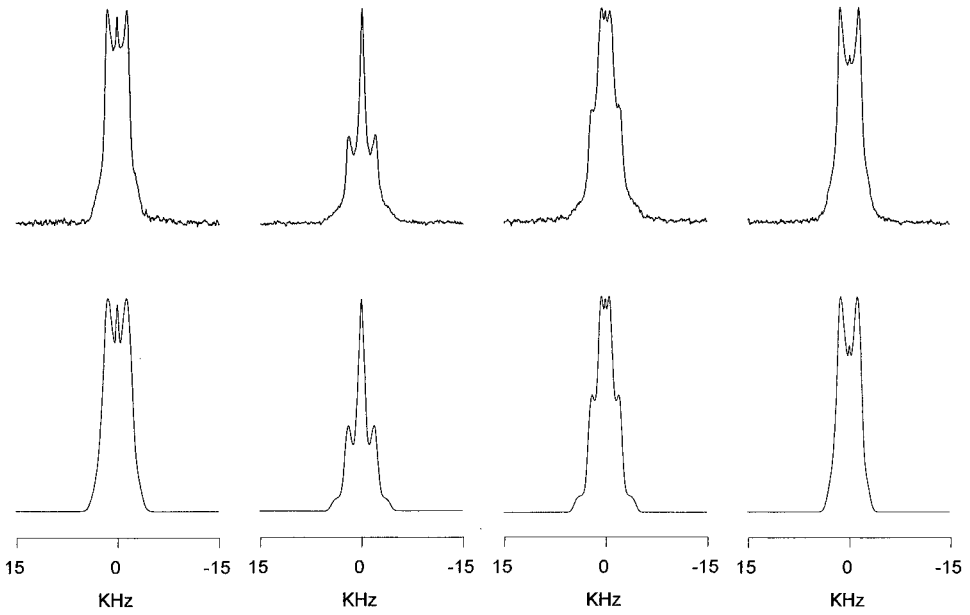

FIGURE 4: ^{2}H NMR spectra of mixed DODAP + POPC-α-d_2 (10/90) cationic lipid bilayers as a function of added PSSS in amounts corresponding to, from left to right, 0, 0.75, 1.0, and 2.0 equiv of PSSS anionic charge to DODAP cationic charge. The top row of spectra are obtained experimentally, while the bottom row are the corresponding computer simulations.

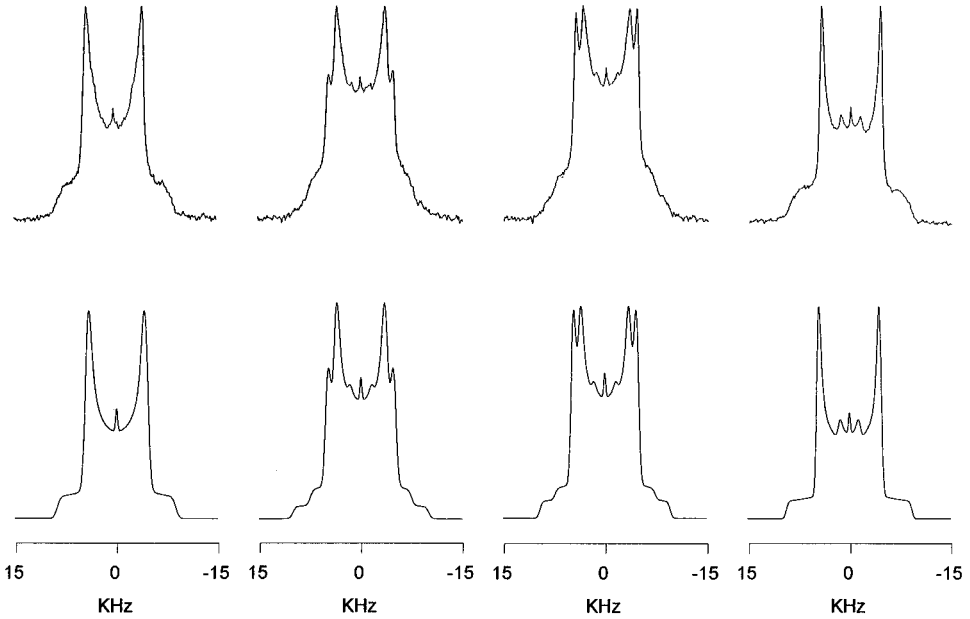

FIGURE 5: ^{2}H NMR spectra of mixed DODAP + POPC-β-d_2 (20/80) cationic lipid bilayers as a function of added PSSS in amounts corresponding to, from left to right, 0, 0.75, 1.0, and 2.0 equiv of PSSS anionic charge to DODAP cationic charge. The top row of spectra are obtained experimentally, while the bottom row are the corresponding computer simulations.

that so form. Nevertheless, over the range of polyelectrolyte concentrations at which resolution of two spectral components is possible, it is evident that with increasing polyelectrolyte levels the quadrupolar splitting from both POPC-α-d_2 and POPC-β-d_2 contained in the polyelectrolyte-free domain trends progressively toward a value characteristic of a neutral membrane surface. In other words, there is a progressive depletion of DODAP from the polyelectrolyte-free domains as polyelectrolyte is added. Conversely, the quadrupolar splitting from both POPC-α-d_2 and POPC-β-d_2 in the polyelectrolyte-bound domains is characteristic of an environment with a high cationic surface charge. This finding appears contradictory, in that the polyelectrolyte-bound domain would be expected to have a surface charge neutralized relative to the initial cationic surface charge. The observed quadrupolar splittings in the polyelectrolyte-bound domain, nevertheless, can be explained rationally, but we defer such a discussion until a later section. For the moment, we remark that the observed quadrupolar splittings are consistent with an enrichment of the polyelectrolyte-bound domains with the cationic DODAP. With increasing polyelectrolyte the quadrupolar splittings tend toward the values characteristic of the control cationic bilayers in the absence of polyelectrolyte. While there are differences to be noted between the responses to different polyelectrolytes, a proper analysis must take into account not just the quadrupolar splitting but also the relative intensities of the two POPC populations.

Quantifying Domain Separation and Domain Composition from ^{2}H NMR Spectra. The ^{2}H NMR spectra obtained in these instances may be analyzed to reveal both the degree of domain separation and the composition of the various domains. The global composition of zwitterionic (X_z^t) or cationic (X_+^t) lipid is defined in mole fractions according to

$$X_z^t + X_+^t = 1 \quad (1)$$

Each such lipid population may be subdivided into those which are polyelectrolyte-bound (superscript b) and those which are polyelectrolyte-free (superscript f), according to

$$\begin{aligned} X_z^t &= X_z^b + X_z^f \\ X_+^t &= X_+^b + X_+^f \end{aligned} \quad (2)$$

The ratio of POPC in the polyelectrolyte-bound versus polyelectrolyte-free domains (X_z^b/X_z^f) at any given level of added polyelectrolyte is equal to the intensity ratio of the two components in the corresponding ^{2}H NMR spectrum as obtained directly from the spectral simulations.

The DODAP content of the polyelectrolyte-free domain is readily obtained from the quadrupolar splitting of the corresponding component in the ^{2}H NMR spectrum via

$$\Delta\nu^f = \Delta\nu_0 + m_i\left(\frac{X_+^f}{X_+^f + X_z^f}\right) \quad (3)$$

where $\Delta\nu_0$ is the quadrupolar splitting measured for 100% POPC and m_i is a calibration constant for a particular charged species and a particular deuterolabeling position in POPC. Previously, we have shown that for DODAP m_i equals -21.2 kHz for POPC-α-d_2 and $+11.5$ kHz for POPC-β-d_2 (Mitrakos & Macdonald, 1996). Equation 3 is readily rearranged to yield directly the desired quantity X_+^f in terms of known and/or experimentally measured quantities:

$$X_+^f = X_z^f\left(\frac{\Delta\nu^f - \Delta\nu_0}{m_i - \Delta\nu^f + \Delta\nu_0}\right) \quad (4)$$

Finally, the amount of DODAP contained within the polyelectrolyte-bound phase is obtained by simple subtraction, according to

$$X_+^b = 1 - X_+^f - X_z^b - X_z^f \quad (5)$$

Note that all four undetermined quantities in eq 2 are obtained without specific reference to the quadrupolar splitting measured for POPC-α-d_2 or POPC-β-d_2 in the polyelectrolyte-bound domain. This domain consists of a ternary mixture of zwitterionic, cationic, and anionic species. As noted earlier, the quadrupolar splittings in the polyelectrolyte-bound domain behave in an apparently contradictory fashion and require a particular delicacy in their interpretation, a pleasure that will be deferred for the moment.

Figure 7 illustrates the manner in which the fraction of total DODAP (X_+^b/X_+^t) or POPC (X_z^b/X_z^t) bound to polyelectrolyte varies as a function of the polyelectrolyte/DODAP charge ratio for the three polyelectrolytes PSSS, PACA and PGLU, as calculated using eqs 1−5. There is a near-linear dependence of the fraction of bound lipid on the level of added polyelectrolyte for both DODAP and POPC for all three polyelectrolytes. For bilayers consisting of mixed DODAP + POPC (10/90), shown in Figure 7A, each equivalent of polyelectrolyte anionic charge binds only approximately 0.75 equiv of DODAP cationic charge, regardless of whether the polyelectrolyte is PSSS, PACA, or PGLU. On the other hand, for bilayers consisting of mixed DODAP + POPC (20/80), shown in Figure 7B, each equivalent of polyelectrolyte anionic charge binds virtually

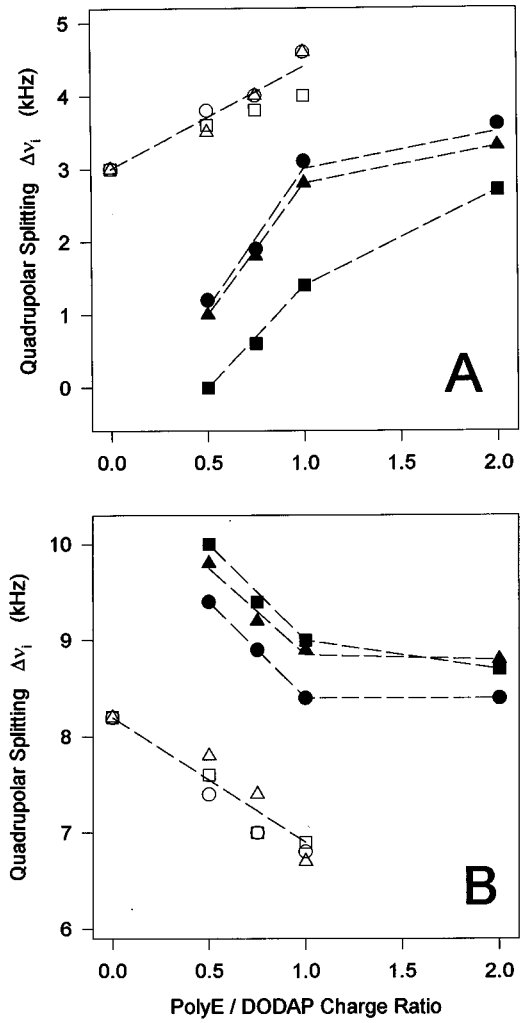

FIGURE 6: ^{2}H NMR quadrupolar splittings of the component Pake doublets in the ^{2}H NMR spectra of mixed DODAP + POPC cationic lipid bilayers as a function of the amount of added polyelectrolyte: PSSS (squares), PACA (circles), and PGLU (triangles). Open symbols refer to the polyelectrolyte-free domain, while solid symbols refer to the polyelectrolyte-bound domain. In panel A the bilayers were composed of DODAP + POPC-α-d_2 (10/90), while in panel B the bilayers were composed of DODAP + POPC-β-d_2 (20/80).

1.0 equiv of DODAP cationic charge, again independent of the detailed chemical structure of the particular polyelectrolyte. In polyelectrolyte−surfactant complexes, there is a critical micellar surface charge density that must be exceeded before the entropic cost of forming a closely surface-bound 1:1 anionic polyelectrolyte/cationic amphiphile complex is outweighed by coulombic forces of attraction (Dubin *et al.*, 1989). This effect might explain the apparent nonstoichiometric anion:cation ratios for the DODAP + POPC (10/90) case.

For POPC, the fraction trapped within the polyelectrolyte-bound domains always lags behind the amount of DODAP. This is consistent with an enrichment of the polyelectrolyte-bound domains with DODAP and a concomitant depletion of the polyelectrolyte-free domains.

The DODAP composition of the polyelectrolyte-free and polyelectrolyte-bound domains as derived from the ^{2}H NMR data is illustrated in Figure 8. The progressive depletion of DODAP out of the polyelectrolyte-free domain with added polyelectrolyte is particulary evident, as is its enrichment within the polyelectrolyte-bound domain. The DODAP composition of the polyelectrolyte-bound domain is not

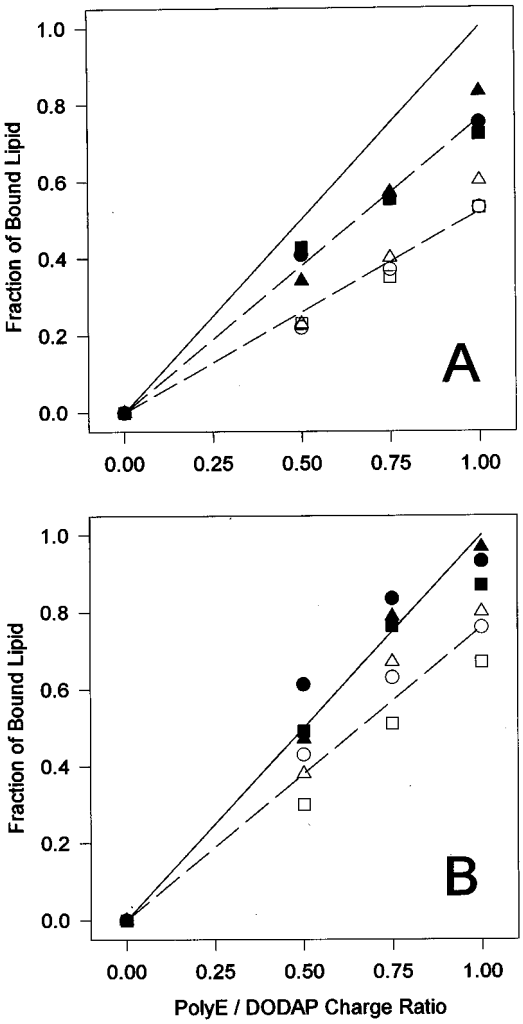

FIGURE 7: Fraction of polyelectrolyte-bound DODAP (X_+^b/X_+^t) or POPC (X_z^b/X_z^t) as a function of the amount of added polyelectrolyte: PSSS (squares), PACA (circles), and PGLU (triangles). Open symbols refer to POPC and show the fraction of the total intensity of the relevant ^{2}H NMR spectrum in the spectral component identified as corresponding to the polyelectrolyte-bound domain. Solid symbols refer to DODAP and show the results of applying eqs 1−5 as described in the text. In panel A the bilayers were composed of DODAP + POPC-α-d_2 (10/90), while in panel B the bilayers were composed of DODAP + POPC-β-d_2 (20/80). The solid line shows the result expected for 1:1 polyelectrolyte/lipid reference binding.

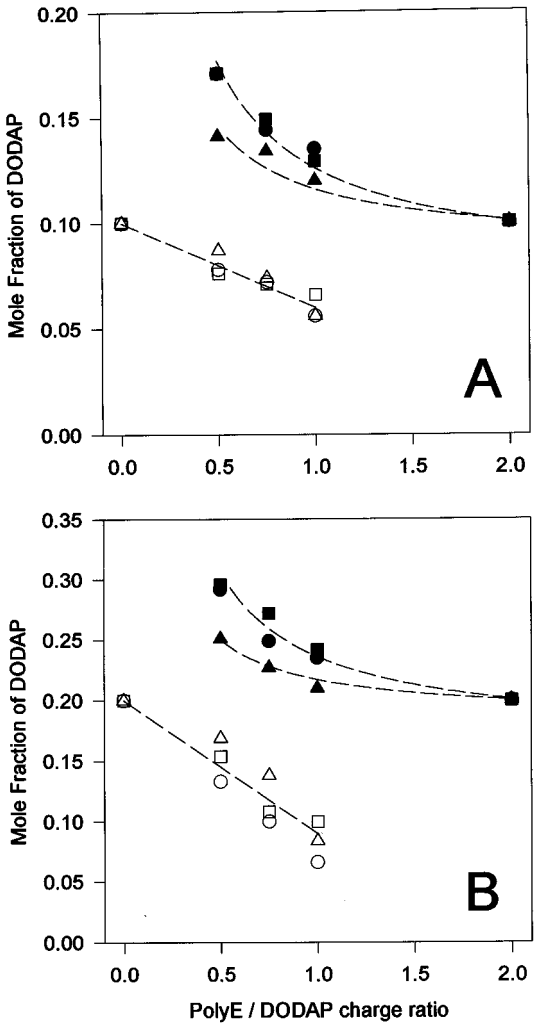

FIGURE 8: Composition of the polyelectrolyte-free and polyelectrolyte-bound domains in mixed DODAP + POPC bilayers as a function of the amount of added polyelectrolyte: PSSS (squares), PACA (circles), and PGLU (triangles). Open symbols are for polyelectrolyte-free domains, while solid symbols are for polyelectrolyte-bound domains. A, DODAP + POPC-α-d_2 (10/90); B DODAP + POPC-β-d_2 (20/80).

constant with increasing polyelectrolyte but rather approaches the initial composition as the membrane surface becomes saturated with polyelectrolyte. Differences between the behavior of different polyelectrolytes are now quite evident. The polyelectrolyte least capable of segregating DODAP into polyelectrolyte-bound domains is PGLU, the least hydrophobic of the three polyelectrolytes. PSSS, the most hydrophobic polyelectrolyte, exhibits the greatest tendency to segregate DODAP. Thus, the propensity to segregate cationic amphiphiles correlates with the potential of the polyelectrolyte to penetrate into the bilayer interior.

^{2}H NMR "Antivoltmeter" Response of POPC in Polyelectrolyte-Bound Domains. The analysis presented above makes no specific reference to the quadrupolar splitting of POPC in the polyelectrolyte-bound domain and relies only on that of the polyelectrolyte-free domain and the ratio of the spectral intensities of the two Pake doublets composing the ^{2}H NMR spectrum. In fact the quadrupolar splitting from both POPC-α-d_2 and POPC-β-d_2 in the polyelectrolyte-bound domain behaves in a fashion precisely opposite to that which one expects from the established "molecular voltmeter" response in either binary or ternary mixtures of charge species. Hence, we have dubbed this response the "Antivoltmeter". Identical behavior has been observed when DNA associates with cationically charged bilayer surfaces (Mitrakos & Macdonald, 1996), or when a cationic polyelectrolyte binds to an anionic bilayer surface (Crowell & Macdonald, 1997). This appears, therefore, to be a generalized polyelectrolyte response as opposed to one specific to a particular polyelectrolyte. In the following we present a rationale for the ^{2}H NMR "Antivoltmeter" and describe the means by which it may be exploited to characterize the polyelectrolyte-bound domains.

In a binary lipid mixture, such as the DODAP + POPC mixture of the polyelectrolyte-free domains, relating the observed quadrupolar splitting from either POPC-α-d_2 or POPC-β-d_2 to the mole fraction of charged lipid is a rather straightforward process involving application of a calibration relation such as eq 3. In ternary mixtures of zwitterionic + cationic + anionic amphiphiles, on the other hand, it has been found empirically that eq 6 may be used:

$$\begin{aligned}(\Delta\nu_{+/-} - \Delta\nu_0) &= (\Delta\nu_+ - \Delta\nu_0) + (\Delta\nu_- - \Delta\nu_0) \\ &= m_+ X_+ + m_- X_-\end{aligned} \tag{6}$$

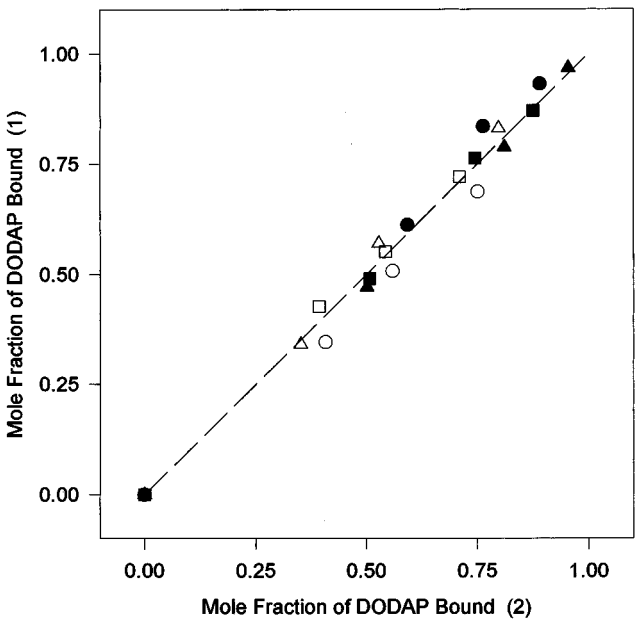

FIGURE 9: Comparison of the two methods of calculating the mole fraction of DODAP bound in the polyelectrolyte-bound domain. Method 1 employs eqs 1−5 and utilizes only the quadrupolar splitting of the polyelectrolyte-free domain plus the intensity ratios of the two components in the ^{2}H NMR spectrum. Method 2 employs eq 6 as applied to the quadrupolar splitting of the polyelectrolyte-bound domain with the assumption that the calibration constant for the polyelectrolyte equals zero. The dashed line shows the result expected for a 1:1 correspondence betweeen the two methods. Open symbols: POPC-α-d_2; Closed symbols, POPC-β-d_2; PSSS (squares), PACA (circles), and PGLU (triangles).

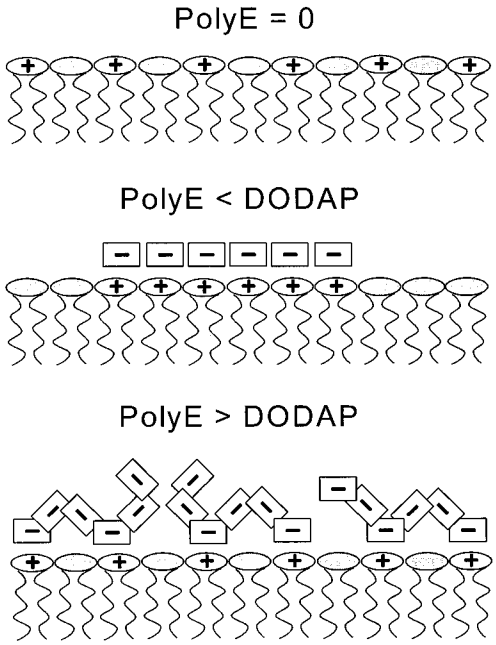

FIGURE 10: Schematic representation of a mixed cationic + zwitterionic lipid bilayer exposed to anionic polyelectrolytes. Only one monolayer of the bilayer is represented. In the absence of polyelectrolyte the cationic and zwitterionic lipids mix such that on average each experiences an identical charge environment. When anionic polyelectrolyte is added in an amount below the anion/cation equivalence point, there is a cationic lipid charge for each anionic polyelectrolyte charge and the polyelectrolyte lies flat on the surface. When anionic polyelectrolyte is added in an amount exceeding the anion/cation equivalence point, the polyelectrolyte can no longer lie flat on the surface and the domain structure disappears.

where $\Delta\nu_{+/-}$ is the quadrupolar splitting of POPC in the ternary mixture, $\Delta\nu_0$ is the quadrupolar splitting for 100% POPC, $\Delta\nu_+$ and $\Delta\nu_-$ are the respective quadrupolar splittings of POPC in cognate binary mixtures with the cationic species of mole fraction X_+ or the anionic species of mole fraction X_-, while m_+ and m_- are the corresponding calibration constants relating the composition to the quadrupolar splitting (Marassi & Macdonald, 1992). In order to apply eq 6 one must have knowledge of the calibration constants in the cognate binary mixtures.

Polyelectrolytes such as those studied here exhibit little if any binding to 100% POPC lipid bilayers so that an independent determination of m_- in eq 6 is not readily achieved. One is forced, therefore, to make judicious assumptions. What if m_- is simply equal to zero? Then eq 6 reduces to eq 3 and the DODAP content of the polyelectrolyte-bound domain is obtained directly from the quadrupolar splitting of the corresponding spectral component. The only reliable check of the validity of any such assumption is to compare the DODAP composition so calculated with that obtained using eqs 1−5. Figure 9 shows exactly such a comparison for all three polyelectrolytes and all polyelectrolyte/DODAP ratios investigated here. Clearly there is a virtual 1:1 correlation between the two methods of calculating X_+[b], indicating the validity of assuming that m_- in eq 6 equals 0.

How might one rationalize the finding that, apparently, POPC does not respond directly to the presence of the polyelectrolyte but only indirectly through the effects of the polyelectrolyte on the distribution of oppositely charged amphiphiles? Two possibilities occur immediately. First, it is conceivable that POPC never encounters the polyelectrolyte directly due to the overwhelming preference of the charged polyelectrolyte for the oppositely charged amphiphile, which effectively blocks access. Second, it is possible that the plane of binding of the polyelectrolyte lies too far above that of the phosphocholine group to interact directly. While currently we cannot decide between these, or other, possible explanations of the "antivoltmeter" response, it should be possible to differentiate between them using nuclear Overhauser enhancement (NOE) NMR measurements.

A Model of Polyelectrolyte-Induced Domains in Lipid Bilayers. In the following we present a schematic picture of polyelectrolytes bound at a lipid bilayer surface, as synthesized from the ^{2}H NMR data presented here. We indicate, further, the information provided by the ^{2}H NMR data regarding domain size, and we highlight some predictions arising from the model and how these might be verified experimentally.

In the absence of polyelectrolyte the binary DODAP + POPC lipid combination is randomly mixed. Lateral diffusion of individual lipids within the plane of any one monolayer of the lipid bilayer averages out any local fluctuations from the global average composition during the time course of a ^{2}H NMR measurement. Consequently, every POPC molecule experiences an identical DODAP composition, as represented schematically at the top of Figure 10. In the ^{2}H NMR spectrum this situation produces a single well-defined quadrupolar splitting, indicating that all POPC molecules report an identical surface charge.

When anionic polyelectrolyte is added in an amount below the global anion/cation equivalence point, there is quantitative binding of polyelectrolyte to the bilayer surface as a result of coulombic attraction. As deduced from the ^{2}H NMR data,

each anionic monomeric unit of the polyelectrolyte couples with a cationic DODAP to produce a 1:1 anion/cation complex, provided there is sufficient initial surface charge density. This indicates that the polyelectrolyte lies flat along the bilayer surface under these circumstances, as represented by the middle scheme in Figure 10. Within the region defined by the presence of polyelectrolyte there is an enrichment with respect to DODAP, maintained over time, again, by the coulombic attraction between amphiphile and polyelectrolyte. Concomitantly, there is a depletion of DODAP from other regions. POPC fortuitously trapped within the polyelectrolyte's domain reports the local excess of DODAP charge versus the depleted charge in other regions of the bilayer. Thus, the ^{2}H NMR spectrum of choline-deuterated POPC reports two separate surface charge environments corresponding to the distinct domains defined by the presence or absence of polyelectrolyte.

When anionic polyelectrolyte is added in an amount above the global anion/cation equivalence point, binding is no longer quantitative and individual polyelectrolytes must compete for cationic surface charges. Since there are fewer of these than there are anionic monomeric units, the polyelectrolyte can no longer lie flat along the surface but instead contacts the surface only intermittently, as shown schematically at the bottom of Figure 10. Since interpolyelectrolyte charge repulsion will cause the polyelectrolytes to distribute more or less evenly over the bilayer surface, the DODAP molecules likewise tend to distribute evenly. This situation produces a single common environment for all amphiphiles and, consequently, a single quadrupolar splitting for choline-deuterated POPC with a value approximating that of the initial conditions in the absence of polyelectrolyte.

The surface area of an individual polyelectrolyte-induced domain can be obtained by summing the surface areas of the amphiphiles constituting such a domain, as extracted from the ^{2}H NMR data. Table 1 shows the number of amphiphiles bound per polyelectrolyte in the polyelectrolyte-defined domain, as a function of the amount of added polyelectrolyte, for each of the three polyelectrolytes investigated here and for the two different DODAP compositions. As noted previously, there is a 1:1 cation/anion ratio in the polyelectrolyte-bound domain for all three polyelectrolytes, at least for the bilayers containing 20% DODAP (and not far removed from this for bilayers containing 10% DODAP).

The data in Table 1 reveal, in addition, that the total number of POPC trapped within the polyelectrolyte-bound domain is much greater for the 10% DODAP than the 20% DODAP bilayers, and this holds for all three polyelectrolytes. Thus, higher initial surface charge densities produce much more compact domains. This is possible because the polyelectrolyte bound at the surface is essentially a two-dimensional random coil capable of expanding and contracting in two dimensions as conditions warrant. Generally, with increasing anion/cation charge ratio, the domain size likewise tends to increase. This effect can be understood by imagining the circumstances encountered by the last of many polyelectrolytes to bind to the surface. Those already bound have depleted the DODAP from the remaining polyelectrolyte-free regions. The next to bind faces a reduced surface charge density producing, as noted above, a more expanded polyelectrolyte-defined domain upon binding to the surface.

Equally revealing is a comparison of the POPC/DODAP ratio in the polyelectrolyte-defined domains for the three different polyelectrolytes. For the 20% DODAP bilayers this ratio falls between approximately 2:1 and 3:1 for PSSS and PACA but increases to between 3:1 and 4:1 for PGLU. Thus, the most hydrophilic of the polyelectrolytes forms the largest domains, encompassing the most POPC molecules.

Table 1: Number of Amphiphiles per Polyelectrolyte in Polyelectrolyte-Bound Domain[a]

anion/cation	DODAP	POPC	total
	DODAP + POPC-α-d_2 (10/90)		
	PSSS (340)		
0.50	290	1405	1695
0.75	250	1430	1680
1.00	245	1655	1900
	PACA (320)		
0.50	260	1260	1520
0.75	235	1410	1445
1.00	240	1540	1780
	PGLU (550)		
0.50	375	2285	2660
0.75	420	2700	3120
1.00	455	3350	3805
	DODAP + POPC-β-d_2 (20/80)		
	PSSS (340)		
0.50	335	795	1130
0.75	340	910	1250
1.00	300	940	1240
	PACA (320)		
0.50	320	775	1095
0.75	320	960	1280
1.00	295	965	1260
	PGLU (550)		
0.50	520	1545	2065
0.75	550	1875	2425
1.00	530	2000	2530

[a] The number in parentheses after the polyelectrolyte abbreviation is the nominal monomers per chain.

The ^{2}H NMR results provide no direct information on whether or not individual domains, as defined by a single polyelectrolyte chain, aggregate into larger patches on the membrane surface. Such patches are well recognized from fluorescence digital imaging microscopy studies of both model and natural membranes (Glaser, 1992). Based upon the size of an individual domain, and asssuming that lipid lateral diffusion within such a domain is the same as in the bulk bilayer, the average lipid's lifetime within one such domain would be far less than 1 ms, the approximate time scale defined by the inverse of the difference between the quadrupolar splittings in the two domains. This suggests that aggregation of individual domains into patches must occur before their existence can be observed via ^{2}H NMR. However, one expects lateral diffusion within the polyelectrolyte-defined domain to be slower than in the bulk, due to the archipelago effect (Saxton, 1993). Clearly, it would be extremely useful to measure the lateral diffusion coefficients for lipids trapped within the polyelectrolyte-defined domain.

The ^{2}H NMR approach described here likewise provides little information regarding domain formation at polyelectrolyte/DODAP charge ratios less than 0.5, due to the small amounts of POPC trapped within the polyelectrolyte-defined domains when there is excess DODAP. A more fruitful approach in this regime might involve observing the DODAP itself. One of the major variables not investigated here is the ionic strength, and it will certainly be of interest to explore domain formation as a function of salt concentration.

The studies reported here yield several predictions amenable to experimental verification. First, if hydrophobic polyelectrolytes embed more deeply into the lipid bilayer than hydrophilic polyelectrolytes, this should be revealed by NOE measurements. Moreover, one would predict that a more superficial binding would produce different polyelectrolyte segmental dynamics, possibly manifest in differences in NMR relaxation times. Second, if polyelectrolytes undergo a transition from a flattened conformation below the equivalence point to one involving loops-and-trains above the equivalence point, this likewise has consequences for the polyelectrolyte's segmental dynamics that might be revealed via NMR relaxation time measurements. Third, the altered polyelectrolyte surface profile above versus below the equivalence point should influence vesicle size as revealed by dynamic light scattering.

REFERENCES

Alderman, D. W., Solum, M. S., & Grant, D. M. (1986) *J. Chem. Phys. 84*, 3717.

Aloy, M. M., & Rabout, C. (1913) *Bull. Soc. Chim. Fr. 13*, 457.

Aneja, R., Chada, J. S., & Davies, A. P. (1970) *Biochim. Biophys. Acta 218*, 102.

Bennet, V. (1985) *Annu. Rev. Biochem. 54*, 273.

Blasie, J. K., Herbette, L., & Pachene, J. (1985) *J. Membr. Biol. 86*, 1.

Bloom, M., & Thewalt, J. L. (1995) *Mol. Membr. Biol. 12*, 9.

Crowell, K. J., & Macdonald, P. M. (1997) *J. Phys. Chem. 101*, 1105.

Cullis, P. R., & de Kruijff, B. (1979) *Biochim. Biophys. Acta 559*, 399.

Davenport, L., Knudson, J., & Brand, L. (1989) in *Subcellular Biochemistry*, (Harriss, J. R., & Etemadi, E. H., Eds.)Vol. 14, p 145, Plenum Press, New York.

Davis, J. H. (1983) *Biochim. Biophys. Acta 737*, 117.

Davis, J. H., Jeffrey, K. R., Bloom, M., Valic, M. I., & Higgs, T. P. (1976) *Chem. Phys. Lett. 42*, 390.

de Kruijff, B., & Cullis, P. R. (1980) *Biochim. Biophys. Acta 602*, 477.

Derjaguin, B. V., & Landau, L. (1941) *Acta Physicochim. URSS 14*, 63.

Dubin, P. L., Thé, S. S., McQuigg, D. W., Chew, C. H., & Gan, L. M. (1989) *Langmuir 5*, 89.

Edidin, M. (1992) *Comments Mol. Cell. Biophys. 8*, 73.

Felgner, P. L., & Rhodes, G. (1991) *Nature 349*, 351.

Glaser, M. (1992) *Comments Mol. Cell. Biophys. 8*, 37.

Harbison, G. S., & Griffin, R. G. (1984) *J. Lipid Res. 25*, 1140.

Haverstick, D. M., & Glaser, M. (1989) *Biophys. J. 55*, 677.

Jesaitis, A. J. (1992) *Comments Mol. Cell. Biophys. 8*, 97.

Jovin, T. M., & Vaz, W. L. C. (1989) in *Methods in Enzymology* (Fleischer, S., & Fleischer B., Eds.) Vol. 172, p 471, Academic Press, New York.

Leventis, R., & Silvius, J. R. (1990) *Biochim. Biophys. Acta 1023*, 124.

Luan, P., Yang, L., & Glaser, M. (1995) *Biochemistry 34*, 9874.

Mabrey, S., & Sturtevant, J. M. (1976) *Proc. Natl. Acad. Sci. U.S.A. 73*, 3862.

Macdonald. P. M., Rydall, J. R., Kuebler, S. C., & Winnik, F. M. (1991) *Langmuir 7*, 2602.

Marassi, F. M., & Macdonald, P. M. (1992) *Biochemistry 31*, 10031.

McElhaney (1982) *Chem. Phys. Lipids 30*, 229.

Mitrakos, P., & Macdonald, P. M. (1996) *Biochemistry 35*, 16714.

Pefferkorn, E. (1995) *Adv. Colloid Interface Sci. 56*, 33.

Rance, M., & Byrd, R. A. (*1983) J. Magn. Reson. 52*, 22.

Saxton, M. J. (1993) *Biophys. J. 64*, 1053.

Seelig, J. (1977) *Q. Rev. Biophys. 10*, 353.

Seelig, J. (1978) *Biochim. Biophys. Acta 515*, 105.

Seelig, J., & Seelig, A. (1980) *Q. Rev. Biophys. 13*, 19.

Seelig, J., Macdonald, P. M., & Scherer, P. G. (1987) *Biochemistry 26*, 7535.

Thompson, T. E., Sankaram, M. B., & Biltonen, R. L. (1992) *Comments Mol. Cell. Biophys. 8*, 1.

Tocanne, J. F. (1992) *Comments Mol. Cell. Biophys. 8*, 53.

Vaz, W. L. C. (1992) *Comments Mol. Cell. Biophys. 8*, 16.

Verwey, E. J., & Overbeek, J. Th.G. (1948) *Theory of the Stability of Lyophobic Colloids*, Elsevier, Amsterdam.

Wolf, D. E. (1992) *Comments Mol. Cell. Biophys. 8*, 83.

Zachowski, A., & Devaux, P. F. (1983) *FEBS Lett. 163*, 245.

BI971324B